USBTU
INTERNATIONAL JOURNAL OF SIVAS UNIVERSITY OF SCIENCE AND TECHNOLOGY
ULUSLARARASI SİVAS BİLİM VE TEKNOLOJİ ÜNİVERSİTESİ DERGİSİ
ISSN:
dergipark.org.tr
DOI:
Araştırma Makalesi / Research Article

Design of a State-Feedback Control System for Sugar Tank Liquid Level Management

Berke Oğulcan PARLAK[1]* (0000-0003-0122-8202)

Hüseyin Ayhan YAVAŞOĞLU[1] (0000-0001-8145-719X)

[1]Yıldız Technical University, Faculty of Mechanical Engineering, Mechatronics Engineering Department, Istanbul

*Sorumlu Yazar (Corresponding author): boparlak@yildiz.edu.tr

Geliş Tarihi (Received): 06.11.2022 **Kabul Tarihi (Accepted)**: 28.12.2022

Abstract

The monitoring and control of the tank liquid level system are indispensable to the sugar production process. By employing advanced control methods such as state feedback, it is possible to obtain a more precise level of control and improve production quality. In this study, four distinct sets of pole locations corresponding to four distinct weighing factors are determined by the symmetric root locus (SRL). Using the Ackermann formula, pole sets are placed. The most successful set is chosen, and the system's steady-state error is reduced to zero by adding a scaling factor. To evaluate the performance of the proposed controller, simulation results for the proportional integral derivative (PID) controller, one of the traditional control methods, and the proposed full-state feedback controller (FSFC) are compared. Time domain specifications are used to optimize the characteristics of the controllers to give the best performance. Optimized FSFC and PID controllers are benchmarked in terms of rise time, settling time, overshoot, peak time, and tracking error. Although both controllers provide zero tracking error, FSFC was found to be more robust and efficient than the PID controller, as FSFC performed better in all other criteria.

Keywords: State Feedback Control, PID Control, Liquid Level, Ackermann, Root Locus

INTRODUCTION

Most industrial processes require precise control methods. Due to the stringent quality standards, the liquid-level system in sugar production is an example of industrial processes requiring sensitive and sophisticated control methods (Ahmad et al., 2020). These control methods can be categorized broadly as conventional, soft, hard, and hybrid (Behrooz et al., 2018).

Typically, conventional methods are ON/OFF and PID methods (Lahlouh et al., 2020). Although the ON/OFF control method provides a fast response, it is ineffective because it accepts only binary input and is inefficient in the long run (Pfeiffer et al., 2014). PID controllers are the most widely employed controller type in the industry, but insufficient gain selection for PID controllers can cause the entire system to be unstable (Song et al., 2015).

Methods using artificial intelligence are referred to as soft control methods. These techniques can be categorized as artificial neural networks (ANN), fuzzy logic (FL), and genetic algorithms (GA). ANN is advantageous due to the good predictability of models and their great performance on nonlinear systems, but they are disadvantageous due to the large amount of data required for accurate results and the lengthy training time required. FL is distinguished by its high precision and speed, and it resembles the human cognitive system (Meje et al., 2020). However, FL control systems are completely reliant on human knowledge and expertise, which is a significant disadvantage. Additionally, FL rules and membership degree may need to be duplicated for greater accuracy. The basis of the GA is derived from the theory of biological evolution (Naidu and Rieger, 2011). In this method, derivatives are not used for optimization, which greatly increases the speed of the method. This is also a drawback of the algorithm, as they may not find the global optimum and may become stuck in the local optimum.

Hard control methods can be examined under four major headings: optimal, robust, adaptive and model predictive control (MPC). Optimal control provides responsive and multivariate control, but its inherent complexity is its biggest drawback. Robust control is advantageous in terms of guaranteeing stability, but requires a good and precise plant model for the implementation and success of the control (Tolaimate and Elalami, 2011). Adaptive control is simple to implement, offers excellent stability and responsiveness, and, like robust control, requires a model of the plant. MPC has advantageous characteristics such as enhancing steady-state response (Rehrl and Horn, 2011), decreasing settling time, rise time and peak time (Huang, 2011), and predicting upcoming disturbing inputs, but it requires an optimization algorithm to do all of this, i.e. it can only be implemented in a computer environment. FSFC can be classified in hard control methods. Most linear techniques become applicable in FSFC. This provides a

great ease of application. FSFC is also preferred for many control applications due to its advantages such as processing speed, zero reference tracking error, and easy placement of the poles as needed.

In the literature, there are numerous studies on the design of conventional, soft, hard and hybrid (using two or more basic controllers together) controllers for liquid level control. In numerous studies, fuzzy proportional derivative (FPD) controller is used as a liquid level control method (Yordanova et al., 2022). Messaouda and Halal (2007) compared the classical proportional derivative controller and FPD controller for two separate liquid level tanks. According to the results, both overshoot and settling time were enhanced with the FPD controller. Basci and Derdiyok (2016) compared the classic proportional integral (PI) controller and adaptive fuzzy controller (AFC) for the liquid level tank. In a system governed by AFC, settling time and overshoot are diminished, tracking error is diminished, and external disturbances are better eliminated. However, since the fuzzy controller does not guarantee stability, the method of trial and error is used to optimize the system. Noel and Pandian (2014) proposed a novel ANN based rapidly exploring random tree (RT) algorithm for constrained high dimensional nonlinear liquid tank level control. The ANN-RT, which has been developed as a new control strategy, performs significantly better than alternative approaches such as PID, FL and MPC in the recent literature, However, it incurs a significant time loss. Engules et al. (2015) studied state-space modeling of the coupled-tank fluid level system and its control with FSFC. Even though the disturbance rejection performance was good, the reference tracking error could not be brought down to zero.

As a contribution to the existing literature, this research proposes a full-state feedback controller for liquid level control for sugar production tank that minimizes reference-tracking error, ensures fast response and easy placement of poles. There is detailed information regarding the modeling and the control steps that are provided. Conventional PID controller that is widely used in the industry and FSFC are compared, and the results are discussed to better comprehend the benefits of the proposed controller.

The mathematical modeling of a sugar production tank system is given in Section 2. In Section 3, FSFC and PID controllers are designed to control the system. Section 4 includes the results of the uncontrolled system, the FSFC-controlled system, and the PID-controlled system. Performance comparison of FSFC and PID controllers is given in Section 5 and the conclusions are drawn in Section 6.

MATHEMATICAL MODELING OF THE SYSTEM

System overview

In this paper, sugar production system from beets is discussed. Initially, a pipe is utilized to transport the beets to the knives, where the beets are completely liquefied. The liquid beets are sucked by a pump and then sprayed into the tank by the electric motor. Figure 1 depicts the overall system architecture.

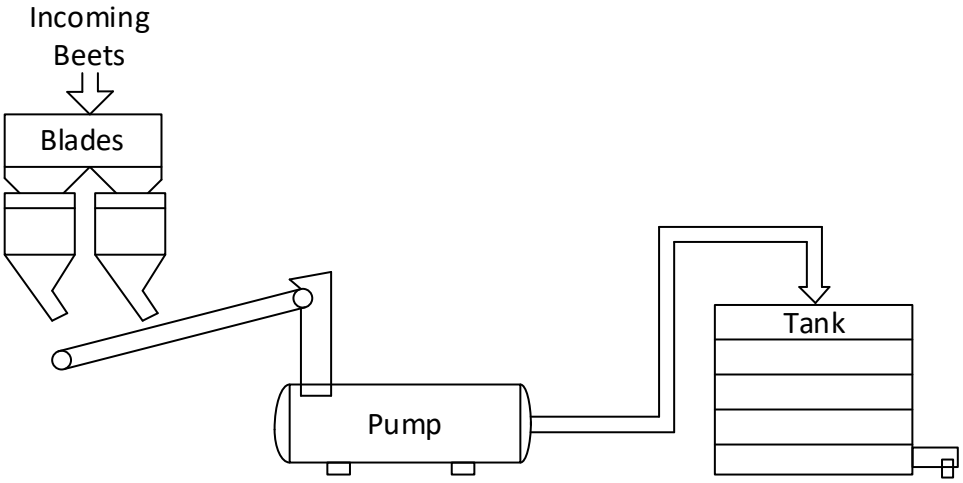

Figure 1. General scheme of sugar beets syrup tank system

Figure 2 illustrates the subdivided into mechanical, electronic, and flow components. This schematic reveal that the pump can operate linearly or nonlinearly based on the pump's component. In this paper, the control strategies will be applied only to the linear system. Mathematical modeling will be conducted according to the system parameters given in Table 1 and Table 2.

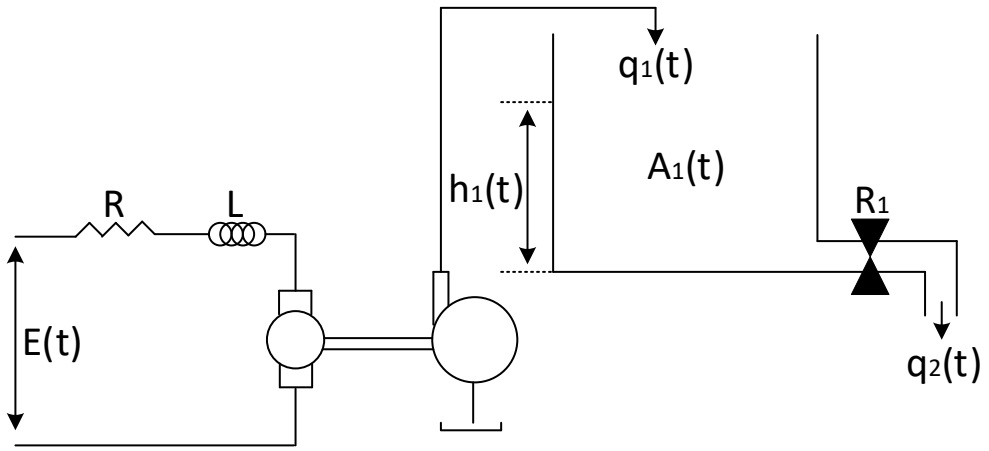

Figure 2. Representation of whole system

Table 1. Parameters of electro–mechanical system

Parameter Name	Value	Unit
L	$19.9*10^{-3}$	H
R	0.973	Ohm
K_m	5.6627	$\frac{Nm}{Amper}$
K_b	6.2	$\frac{Vsec}{Rad}$
J	1.72	kgm^2

Table 2. Parameters of fluid–tank system

Parameter Name	Value	Unit
D_p	20	$\frac{m^3}{rad}$
A_1	10	m^2
R_1	0.06	$\frac{m}{m^3 sec^{-1}}$

The block diagram

The block diagram for an armature-controlled direct current motor is shown in Figure 3. Using this block diagram scheme, the equations of motion of this part can be derived. Next, the relationship between the angular velocity of the motor and the output flow rate of the pump should be examined.

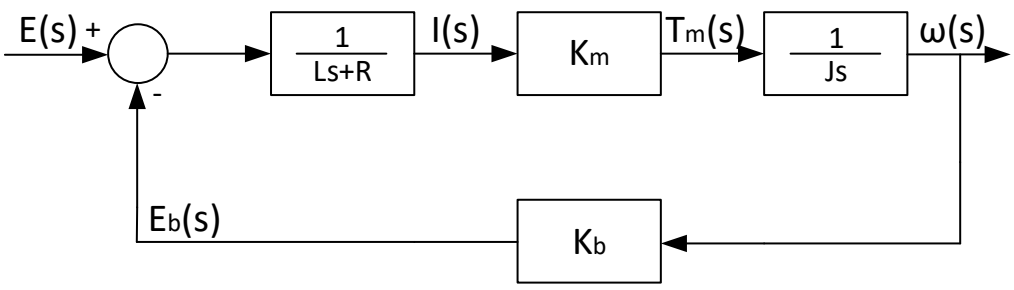

Figure 3. Block diagram of an armature-controlled DC motor

For a laminar flow, the pump's flow rate (q_1) is directly proportional to stroke displacement of the pump (q_p), shaft's angular velocity (w) and pump volumetric efficiency (n_p). Consequently:

$$q_1(t) = q_p * w(t) * n_p \quad (1)$$

Here, the values for pump stroke displacement and pump volumetric efficiency are constant. Thus, the relationship between the motor angular velocity and the flow rate delivered by the pump can be represented by constant (D_p):

$$q_1(t) = D_p * w(t) \text{ since } D_p = q_p * n_p \quad (2)$$

The fluid system has been studied after establishing the relationship between motor angular velocity and pump output flow. The equations of motion for a fluid system are derived using the continuity law. Figure 4 depicts the system's conclusive block diagram.

$$q_1(t) - q_2(t) = A_1 * \frac{dh_1(t)}{dt} \quad (3)$$

$$q_2(t) = h_1(t) * \frac{1}{R_1} \quad (4)$$

If Equation 4 is substituted in Equation 3, flow rate delivered by pump will be

$$q_1(t) = A_1 * \frac{dh_1(t)}{dt} + h_1(t) * \frac{1}{R_1}. \quad (5)$$

Defining the state space matrices

From the block diagram obtained in Figure 3, the relationship between voltage and angular velocity can be written as

$$\frac{K_m}{LJs^2+RJs+K_mK_b} = \frac{W(s)}{E(s)}. \quad (6)$$

If Equation 6 is arranged so that voltage is on one side and angular velocity is on the other, and then the inverse Laplace transform is applied, the voltage will be

$$e(t)K_m = LJ\ddot{w}(t) + RJ\dot{w}(t) + K_mK_bw(t). \quad (7)$$

The relation between W(s) and $H_1(s)$ can be written as follows by looking at the block diagram in Figure 4:

$$W(s)\frac{D_p}{A_1 s+\frac{1}{R_1}} = H_1(s) \tag{8}$$

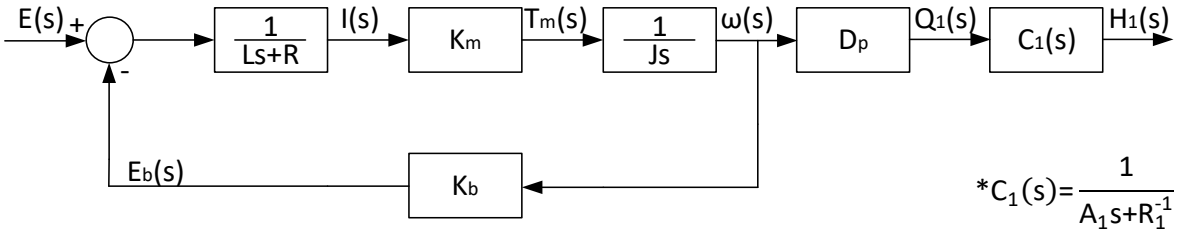

Figure 4. Block diagram of whole system

If Equation 8 is arranged such that liquid level is on one side and angular velocity is on the other, and the inverse Laplace is taken, the angular velocity will be

$$w(t)D_p = A_1\dot{h_1}(t) + \frac{1}{R_1}h_1(t). \tag{9}$$

If state space variables are chosen as

$$\begin{cases} x_1 = h_1(t), \\ x_2 = w(t), \\ x_3 = \dot{w}(t), \\ u = e(t), \end{cases}$$

Equation 7 can be arranged as follows:

$$uK_m = \dot{x_3}LJ + x_3RJ + x_2K_mK_b \tag{10}$$

The derivative of the third state variable can be obtained using Equation 10.

$$\dot{x}_3 = \frac{-K_mK_b}{LJ}x_2 - \frac{R}{L}x_3 + \frac{K_m}{LJ}u \tag{11}$$

The derivative of the first state variable can be obtained by rearranging Equation 9.

$$x_2 D_p = \dot{x}_1 A_1 + \frac{1}{R_1} x_1, \tag{12}$$

$$\dot{x}_1 = \frac{-1}{A_1 R_1} x_1 + \frac{D_p}{A_1} x_2. \tag{13}$$

The derivative of the second state variable is directly equal to the third state variable itself. If the liquid level is selected as a single output, the state space matrices are found as

$$A = \begin{bmatrix} \frac{-1}{A_1 R_1} & \frac{D_p}{A_1} & 0 \\ 0 & 0 & 1 \\ 0 & \frac{-K_m K_b}{LJ} & -\frac{R}{L} \end{bmatrix},$$

$$\mathbf{B} = \begin{bmatrix} 0 \\ 0 \\ \frac{K_m}{LJ} \end{bmatrix},$$

$\mathbf{C} = [1 \quad 0 \quad 0]$ and $\mathbf{D} = 0$.

CONTROL OF THE SYSTEM

State feedback controller

The problem of pole assignment with state feedback and related studies has a significant place in control theory and a lengthy history. The success of pole assignment plays a critical role in stability and system performance. Numerous methods have been developed for pole assignment, and the success, advantages and disadvantages of all these methods according to different performance criteria have been examined by Soylemez (Söylemez and Munro, 1999). In Figure 5 the method is visualized by adding a K gain matrix to the feedback path.

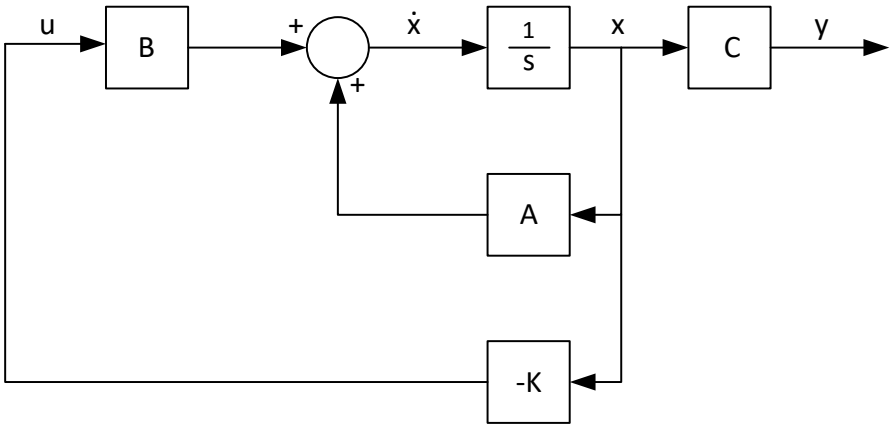

Figure 5. State feedback controller

The necessary and sufficient condition for the application of this method is that the system to be applied is fully controllable. If the controllability matrix of a system is not singular (determinant is not zero), the system is considered controllable. Since the determinant of the controllability matrix calculated according to the values given in Table 1 and Table 2 is -9.0564*10^6, the system is controllable.

Determining the desired characteristic equation via SRL

The objective of the SRL problem is to minimize a performance index. This performance index is defined as $\int_0^\infty [\rho * z^2(t) + u^2(t)] * dt$. Here, while u(t) defines the control effort, z(t) is chosen directly as the system output. The ρ value here is referred to as the weighing factor, which defines the balance between energy consumption and performance of the system. Increasing the ρ value will accelerate the system response and reduce the settling time of the system but will increase the energy consumed in the system. To see the effect of ρ change on the system, four controllers will be designed for different ρ values and system outputs will be compared.

According to the system parameters in Table 1 and Table 2, the open loop transfer function for SRL is determined as

$$G_o(s) = \frac{C_1}{s^6 - C_2\, s^5 - C_3\, s^4 + C_4\, s^3 + C_5\, s^2 - C_6\, s - C_7}, \tag{14}$$

with the constants

$$\begin{cases} C_1 = -1.095 * 10^5, \\ C_2 = 6.395 * 10^{-14}, \\ C_3 = 342, \\ C_4 = 1.1 * 10^{-10}, \\ C_5 = 1.05 * 10^6, \\ C_6 = 7.47 * 10^{-8}, \\ C_7 = 2.923 * 10^6. \end{cases}$$

The SRL drawing of the system is given in Figure 6. Four different sets of poles were determined from this locus. These sets of poles are listed in Table 3.

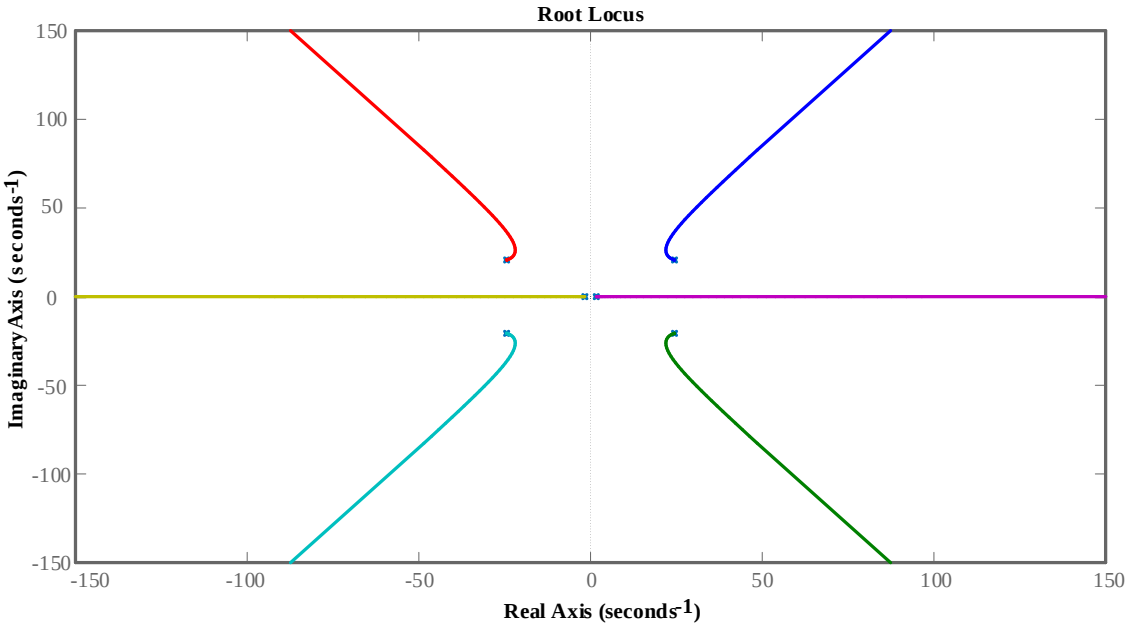

Figure 6. SRL of system

Table 3. Selected poles for different weighing factors

Pole Sets	Weighing Factor	Pole 1	Pole 2	Pole 3
Set – 1	12.2	-24.4 + 20.7i	-24.4 - 20.7i	-100
Set – 2	8570	-21.9 + 25.8i	-21.9 - 25.8i	-100
Set – 3	315000	-29.9 + 48.5i	-29.9 - 48.5i	-100
Set – 4	76700000	-71.8 + 123i	-71.8 - 123i	-100

Application of Ackermann's Formula

To obtain the desired characteristic equation, the plant's feedback must be supplemented with a K matrix. Using Ackermann's formula, the values of this K matrix were determined. Different K matrices have been created for the pole sets given in Table 3. These matrices are given in Table 4.

Table 4. K gain matrices for different pole sets

K matrix
For the 1st set [280.9 28.0 0.59]
For the 2nd set [319.4 25.8 0.56]
For the 3rd set [935.9 47.9 0.66]
For the 4th set [5957.9 200.8 1.2]

Adding a scale factor for zero steady-state error

The steady-state error is the difference between the predetermined input signal and the output signal as time approaches infinity. Approaching this difference to zero is of great importance in control systems. In state space analysis, this is accomplished by adding an N factor in front of the input signal. Figure 7 shows the visualization of the methodology.

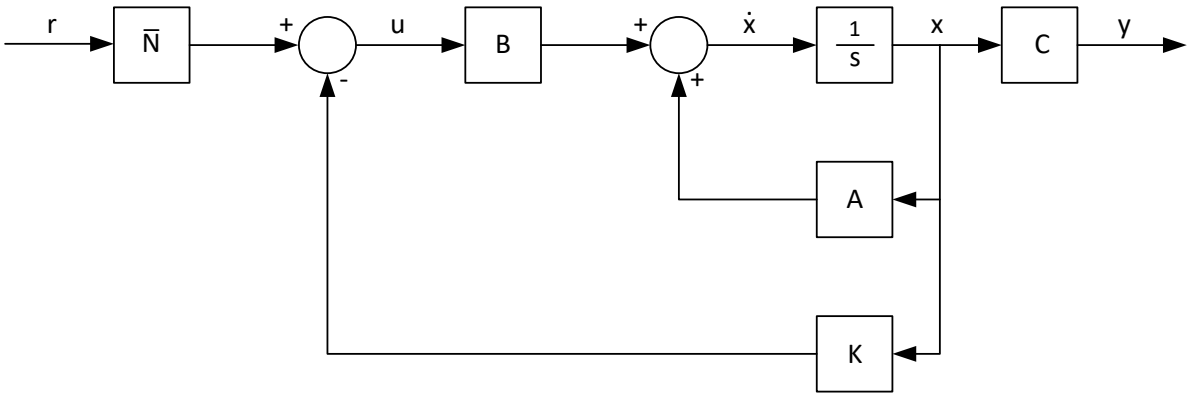

Figure 7. Adding scale factor N to the system

PID controller

PID controllers have a history dating back to the early 20th century. This long history has contributed to their development and made them popular for the industry. Because PID controllers respond quickly and efficiently to changes, they are often used in manufacturing operations where sudden changes can occur. This feature makes them suitable for sugar production tanks. The output of a basic PID structure is given in Equation 15, and the block diagram of the PID controller is given in Figure 8.

$$c(t) = K_p e(t) + K_i \int_0^t e(t) + K_d \frac{de(t)}{dt} \qquad (15)$$

Where e(t) is the error, c is the control signal and K_p, K_i, K_d are proportional, integral and derivative gain constants, respectively.

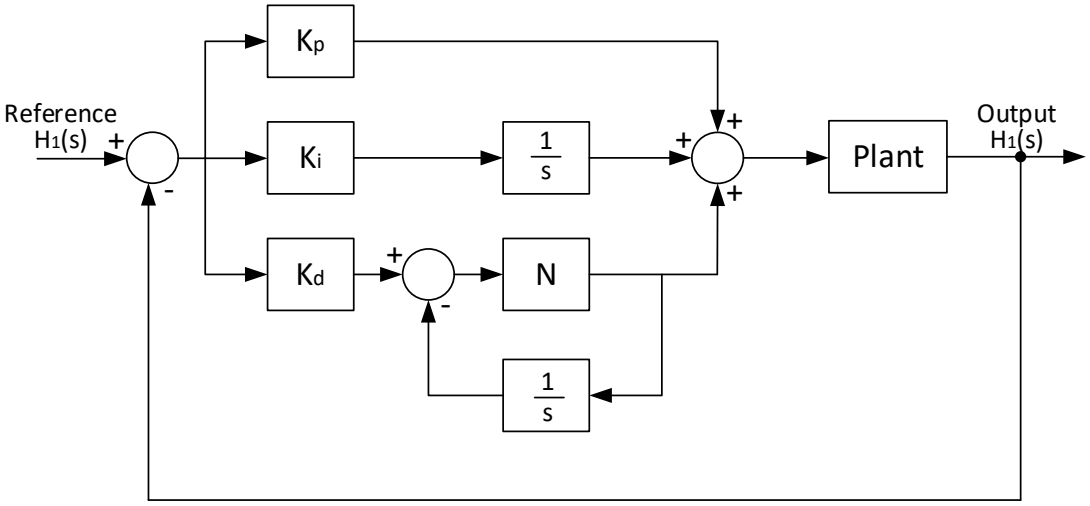

Figure 8. Block diagram of the system with a PID controller

PID controllers typically have three adjustable parameters: proportional, integral, and derivative. These parameters can be modified to optimize the performance of the controller for a particular application. This adjustment process is referred to as tuning. A PID controller can be tuned in a number of different ways. The most common method is called the Ziegler-Nichols method. This involves gradually increasing the output until the system starts to oscillate, and then backing off slightly. Other methods include the Cohen-Coon method and the Tyreus-Luyben method. In the study, 4 different PID gain sets that will give reasonable control performance in terms of rise time, settling time, overshoot, peak time and steady-state error were obtained by using MATLAB PID Tuner. These gain sets are shown in Table 5.

Table 5. The resulting PID gain sets

PID Gain Sets	**K_p**	**K_i**	**K_d**	**N**
Set – 1	39.6639	124.38	0.8097	1403.6638
Set – 2	17.8843	42.2408	0.71982	641.5981
Set – 3	19.8558	60.4766	0.52338	7.0678
Set – 4	82.2228	321.1529	2.3885	2800.6774

RESULTS

Results of uncontrolled system

The output that the uncontrolled sugar production tank system responds to the 12V step input is given in Figure 9, and some time domain specifications for the same input are given in Table

6. Although there is no oscillation in the system, it is clearly seen in the table that the time domain specifications need to be improved.

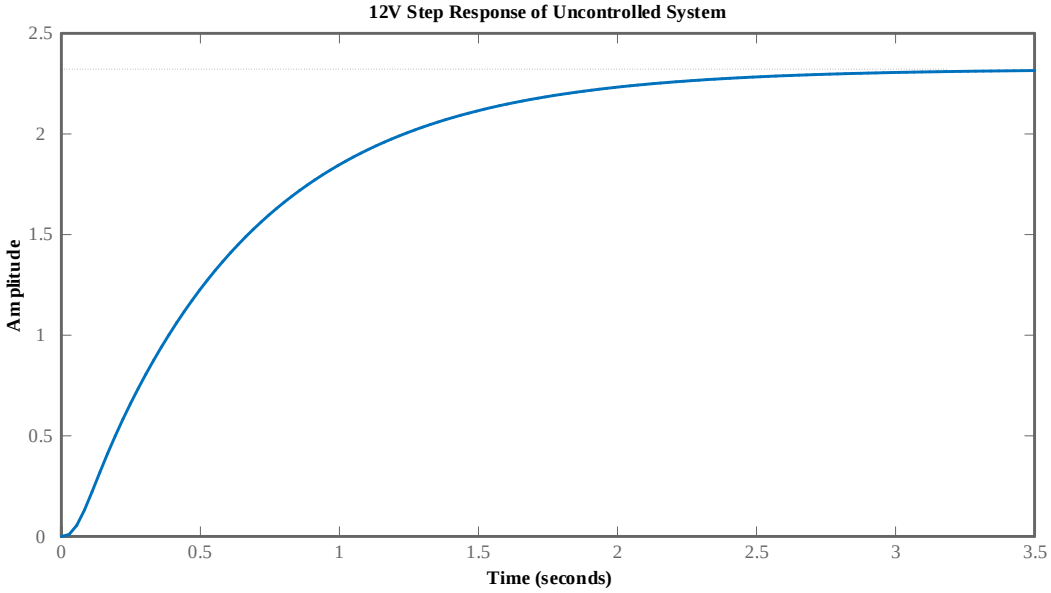

Figure 9. 12V step response of uncontrolled system

Table 6. Time domain specifications of uncontrolled system

Rise Time	Settling Time	Overshoot	Peak Time
1.3164 sec.	2.3953 sec.	0 %	4.3933 sec.

Results of the state feedback controlled system

To determine the impact of the weighing factor on the system, four distinct sets of poles were obtained using four distinct weighing factors. These poles were placed with the Ackermann Formula and four separate K matrices were obtained in Table 4. The 3-meter step input was applied to all sets and the outputs were observed. The outputs of the sets are shown in Figure 10 and the time domain specifications are shown in Table 7.

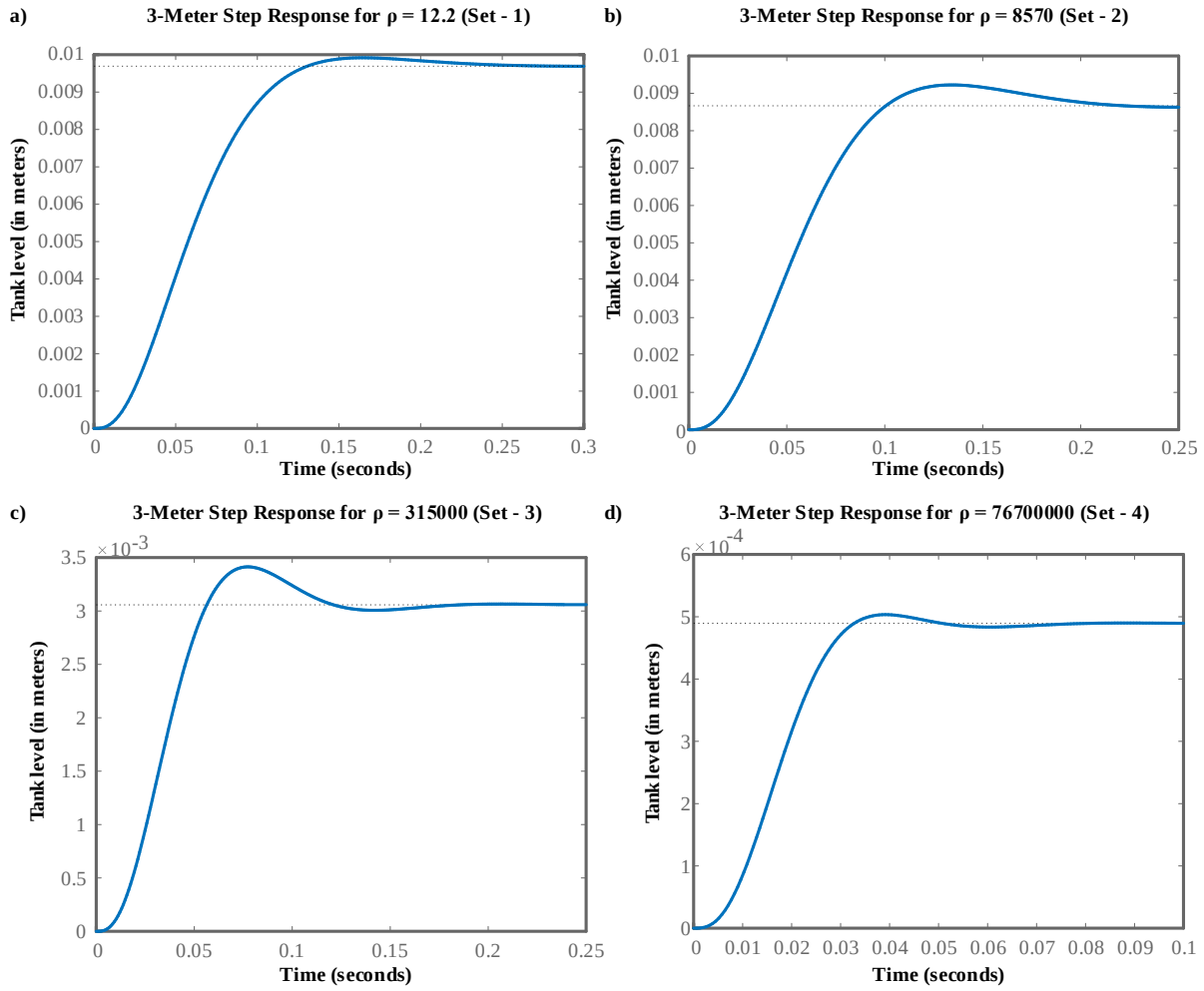

Figure 10. 3-meter step input responses of systems with different weighing factors

Table 7. Time domain specifications of FSFC-controlled systems with different weighing factors

Pole Sets	Weighing Factor	Rise Time (sec.)	Settling Time (sec.)	Overshoot (%)	Peak Time (sec.)
Set – 1	12.2	0.0767	0.1831	2.2944	0.1642
Set – 2	8570	0.0623	0.1881	6.4428	0.1345
Set – 3	315000	0.0348	0.1122	11.6259	0.0774
Set – 4	76700000	0.0192	0.0441	2.8689	0.0391

Results of the PID-Controlled system

To determine the impact of different PID gains on the system, four different PID gain sets given in Table 5 were obtained with reasonable control performance and using the MATLAB PID Tuner. The 3-meter step input was applied to all sets and the outputs were observed. The outputs of the sets are shown in Figure 11 and the time domain specifications are shown in Table 8.

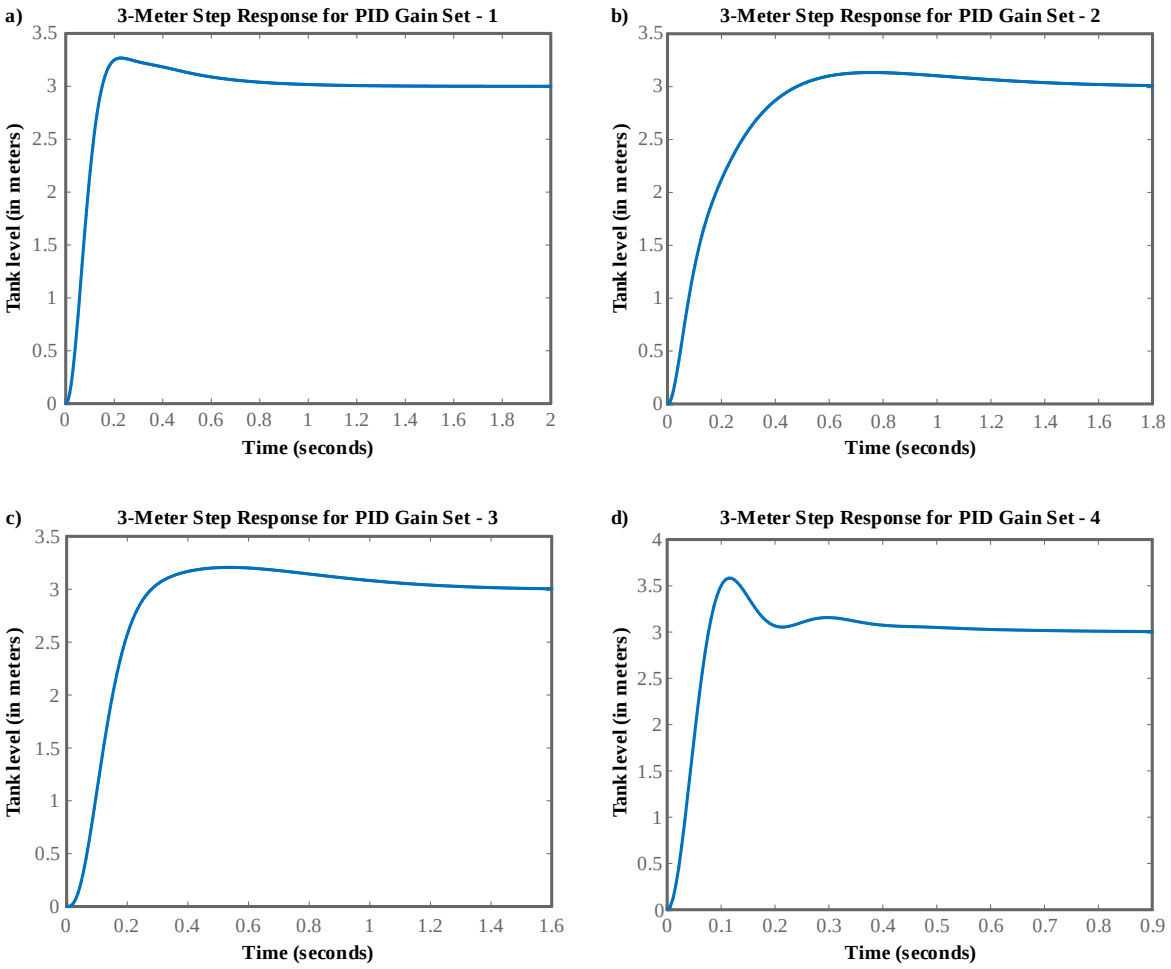

Figure 11. 3-meter step input responses of systems with different PID gains

Table 8. Time domain specifications of PID-controlled systems with different PID gains

PID Gain Sets	Rise Time (sec.)	Settling Time (sec.)	Overshoot (%)	Peak Time (sec.)
Set – 1	0.0977	0.6973	8.9294	0.2296
Set – 2	0.2988	1.2394	4.4590	0.7603
Set – 3	0.1628	1.0926	6.8918	0.5386
Set – 4	0.0513	0.4504	19.4431	0.1135

PERFORMANCE OF PROPOSED FSFC

Comparison with the PID Controller

Considering the results of four distinct sets for the proposed FSFC controller, it was observed that as the weighing factor increased, the specifications of the system such as settling time and rise time improved. However, increasing the weighing factor will increase the energy consumption. Since sugar is an industrial product, energy usage will result in additional

expenses. Therefore, the controller designed for 1st set was chosen for the lowest energy consumption. Despite this controller's excellent settling time, the tracking error is enormous. Therefore, the tracking error is reduced to zero by adding a scaling factor of 309.4313 to the system using the methodology in Figure 7.

When the results of four different sets for the PID controller were evaluated, it was seen that the system with the controller created with the 4th set responds and settles faster. However, the system has a lot of oscillation. Therefore, the first set was picked, as it oscillates less and offers adequate control performance.

The output of the system controlled by two different controllers is given in Figure 12. The tracking error is zero for both controllers. However, looking at the time domain specifications, it can be said that FSFC gives better results than the PID controller in terms of rise time, settling time, peak time and overshoot.

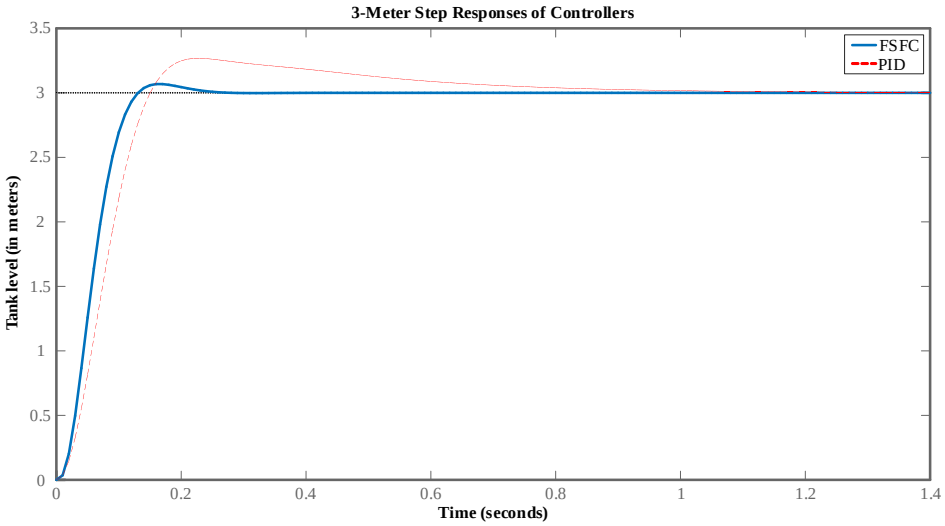

Figure 12. 3-meter step input response of the system controlled by PID controller and FSFC

Experimental verification

The experimental results represent the actual behavior of the tested controller with specific measuring errors, whereas the simulation results represent the same controller's behavior based on its theoretical model. To comprehend the accuracy of the simulation-based proposed system, it is essential to compare the developed systems to the experimental studies in the literature. A system similar to the liquid level tank system discussed in this study was modeled by Mamur et al. (2017) and the control performance of the conventional PID controller was tested in an experimental rig. In the experimental study, the reference inputs given in Table 9 were applied to the liquid level tank system consecutively and the outputs given in Table 10 were obtained.

Table 9. Reference inputs applied in the experimental study

Input Number	Input Type	Input Offset (cm)	Input Amplitude (cm)
1	Step	0.7	0.1
2	Step	0.8	0.1
3	Step	0.9	0.05

Table 10. Outputs obtained from the inputs applied in the experiment

Applied Input	Settling Time (sec.)	Steady-State Error (%)
Input – 1	72	2
Input – 2	5	0
Input – 3	372	0

The least amount of settling time and steady-state error were attained in the experimental study based on input–2. Therefore, the input–2 value in Table 10 was chosen to compare the results of the proposed and experimental systems. To compare the proposed FSFC with the experimental outputs, the tank capacitance and the flow resistance of the pipe are updated according to the experimental system. Due to the changing parameters of the system, the SRL is redrawn. According to the new SRL, poles are determined as –30.9 + 50.4i, –30.9 – 50.4i, and –150 with a weighing factor of 1000. The gain matrix K required to place these poles is calculated as [80.2158 70.9562 0.9847] using Ackermann's formula and a scaling factor of 22667 is added to the system to reduce the tracking error to zero. The output of the proposed controller for the input–2 value is depicted in Figure 13.

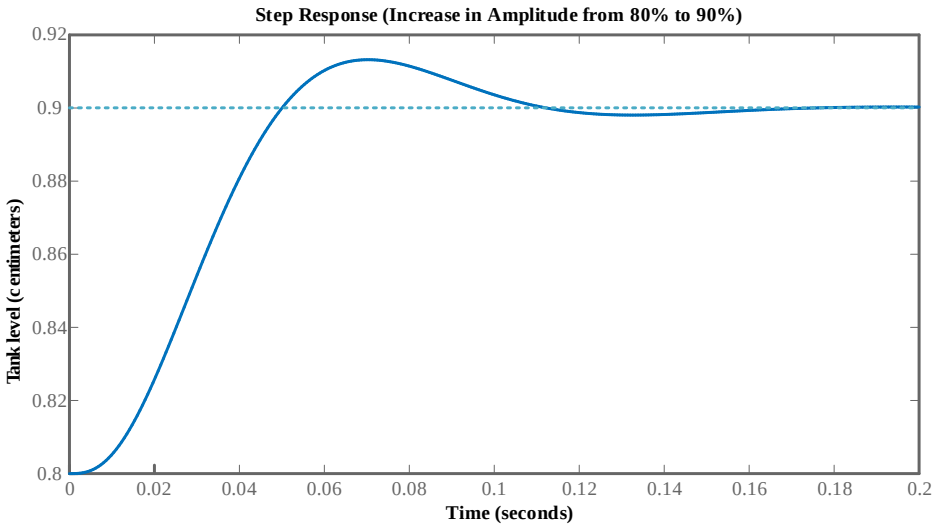

Figure 13. Input – 2 response of the proposed FSFC-controlled system

Nonetheless, simulation studies might not accurately reflect actual conditions. Incorporating an error factor into the calculations could be a viable strategy for achieving a more accurate comparison. To calculate the error factor, the differences between simulation and experimental results obtained with the same parameters and controllers can be examined. Therefore, the system parameters were updated based on the experimental setup, and simulations were conducted using the PID coefficients used in the experiment. The simulation response of the PID-controlled system designed with experimental parameters for input - 2 is shown in Figure 14.

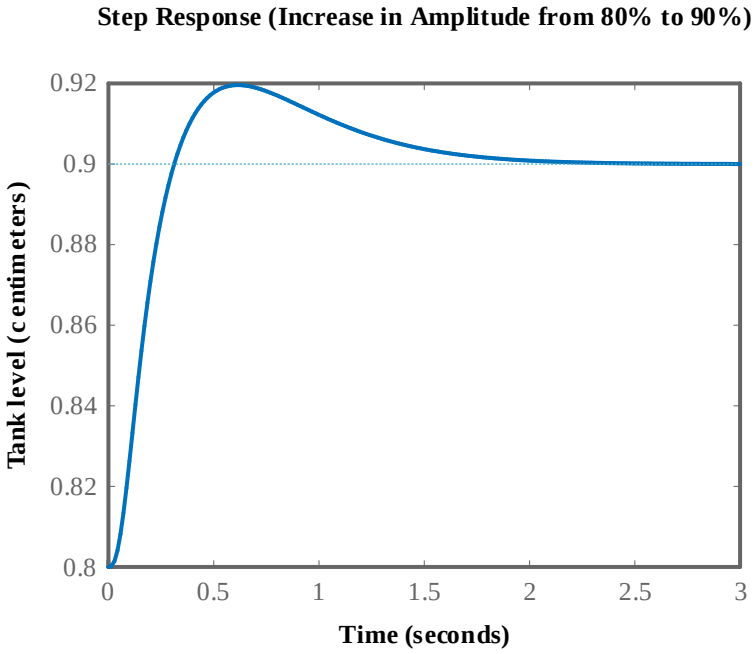

Figure 14. Input – 2 response of the PID-controlled system

While the settling time was 5 seconds in the experiment, it was computed 1.719 seconds in the simulation. Therefore, an error factor of $\in_{\xi} = 2.91$ was obtained to compare the simulation data with the experimental data.

The following details can be provided regarding the experimental and proposed controllers:

- Both controllers have zero tracking errors.
- In contrast to the PID-controlled system, which settles in 5 seconds, the proposed FSFC-controlled system settles in 0.105 seconds.
- Taking into account the 2.91 error factor calculated to bring simulation data closer to reality, the FSFC-controlled system settles in 0.306 seconds as opposed to 0.105 seconds.

Therefore, it can be observed that the proposed FSFC yields better results than the outputs of the experimental study employing the conventional PID controller. However, it should be noted that the settling-time of the proposed controller, which settles significantly faster, will be slightly lengthened when retested using the actual test setup.

CONCLUSIONS

From a material standpoint, industrial operations frequently require swift solutions. PID controllers dominate the market due to their familiarity and ease of application. This is related to the fact that they can be adjusted with only three gain parameters. This advantage can turn into a major weakness, such as the instability of the system in the absence of adequate gain selection. To overcome such critical situations, it is vital to focus on more up-to-date controllers with a solid theoretical basis.

The paper presents state feedback control of the liquid level of a sugar production tank system. Four alternative FSFC designs were made for four different weighing factors with the help of SRL. Comparing the performances of these FSFCs, an improvement in settling and rising times was observed with increasing weighing factor, but this would increase energy consumption. The 1st dataset with the highest energy efficiency has a settling time of 0.1831 seconds, a rise of 0.0767 seconds, and an overshoot percentage of 2.2944. On the other hand, the best-performing PID controller among the four alternative designs has a settling time of 0.6973 seconds, a rise of 0.0977 seconds, and an overshoot percentage of 8.9294. Thus, the proposed FSFC showed a 73.7% improvement in settling time, 21.5% improvement in rising time, and 74.3% reduction in overshoot over conventional PID controller in controlling the liquid level of a tank. The proposed FSFC was also compared with the results of an experimental study on the controlling of a similar liquid level tank system in the literature. The FSFC showed a 93.9% improvement in settling time over the PID controller used in the experimental study. All the improvements clearly showed that for a liquid level control application, the FSFC outperforms the PID controller.

APPENDIX

Abbreviations

AFC Adaptive Fuzzy Controller

ANN Artificial Neural Network

FL Fuzzy Logic

FPD	Fuzzy Proportional Derivative
FSFC	Full State Feedback Controller
GA	Genetic Algorithms
MPC	Model Predictive Control
PI	Proportional Integral
PID	Proportional Integral Derivative
RT	Random Tree
SRL	Symmetric Root Locus

Symbols

A_1	Capacitance of Tank
D_p	Relationship Between q_p and n_p
E	Armature Circuit Voltage
E_b	Motor Back EMF
H_1	Liquid Level Height of Tank
J	Moment of Inertia of the Rotor
K_b	Motor Torque Constant
K_d	Derivative Gain
K_i	Integral Gain
K_m	Electromotive Force Constant
K_p	Proportional Gain
L	Armature Circuit Inductance
N	Derivative Filter Coefficient
n_p	Pump Volumetric Efficiency
q_1	Flow Rate Delivered by Pump
q_2	Flow Rate of Liquid Flowing from the Tank
q_p	Stroke Displacement of Pump
R	Armature Circuit Resistance
R_1	Flow Resistance in the Pipe to the Right of Tank
w	Shaft's Angular Velocity
ρ	Weighing Factor
ϵ_ξ	Error Factor

REFERENCES

Ahmad, S., Ali, S., & Tabasha, R. (2020). The design and implementation of a fuzzy gain-scheduled PID controller for the Festo MPS PA compact workstation liquid level control. *Engineering Science and Technology, an International Journal*, *23*(2), 307–315.

Başçi, A., & Derdiyok, A. (2016). Implementation of an adaptive fuzzy compensator for coupled tank liquid level control system. *Measurement*, *91*, 12–18.

Behrooz, F., Mariun, N., Marhaban, M. H., Mohd Radzi, M. A., & Ramli, A. R. (2018). Review of control techniques for HVAC systems—Nonlinearity approaches based on Fuzzy cognitive maps. *Energies*, *11*(3), 495.

Engules, D., Hot, M., & Alikoc, B. (2015). Level control of a coupled-tank system via eigenvalue assignment and LQG control. *2015 23rd Mediterranean Conference on Control and Automation (MED)*, 1198–1203.

Huang, G. (2011). Model predictive control of VAV zone thermal systems concerning bi-linearity and gain nonlinearity. *Control Engineering Practice*, *19*(7), 700–710.

Lahlouh, I., Rerhrhaye, F., Elakkary, A., & Sefiani, N. (2020). Experimental implementation of a new multi input multi output fuzzy-PID controller in a poultry house system. *Heliyon*, *6*(8), e04645.

Mamur, H., Atacak, I., Korkmaz, F., & Bhuiyan, M. R. A. (2017). Modelling and application of a computer-controlled liquid level tank system. *Computer Science & Information Technology (CS & IT)*, 97–106.

Meje, K., Bokopane, L., Kusakana, K., & Siti, M. (2020). Optimal power dispatch in a multisource system using fuzzy logic control. *Energy Reports*, *6*, 1443–1449.

Messaouda, A., & Halal, F. (2007). Comparative analysis of PD classical control and PD fuzzy control in two liquid level tanks. *IFAC Proceedings Volumes*, *40*(18), 487–491.

Naidu, D. S., & Rieger, C.G. (2011). Advanced control strategies for HVAC&R systems—An overview: Part II: Soft and fusion control. *Hvac&R Research*, *17*(2), 144–158.

Noel, M. M., & Pandian, B. J. (2014). Control of a nonlinear liquid level system using a new artificial neural network based reinforcement learning approach. *Applied Soft Computing*, *23*, 444–451.

Pfeiffer, C.F., Skeie, N.-O., & Perera, D.W.U. (2014). *Control of temperature and energy consumption in buildings-a review.*

Rehrl, J., & Horn, M. (2011). Temperature control for HVAC systems based on exact linearization and model predictive control. *2011 IEEE International Conference on Control Applications (CCA)*, 1119–1124.

Song, Y., Wu, S., & Yan, Y. Y. (2015). Control strategies for indoor environment quality and energy efficiency—a review. *International Journal of Low-Carbon Technologies*, *10*(3), 305–312.

Söylemez, M. T., & Munro, N. (1999). Pole assignment for uncertain systems. *IEE CONTROL ENGINEERING SERIES*, 251–272.

Tolaimate, I., & Elalami, N. (2011). Robust Control Problem as H2 and H∞ control problem applied to the robust controller design of Active Queue Management routers for Internet Protocol. *International Journal of Systems Applications, Engineering & Development*, *6*.

Yordanova, S., Slavov, M., Prokopiev, G., & Stoitseva-Delicheva, D. (2022). Industrial Bound Design and Application of Fuzzy Logic PID Controller for Liquid level in Carbonisation Column. *2022 International Conference Automatics and Informatics (ICAI)*, 210–217.